NATIONAL AERONAUTICS AND SPACE ADMINISTRATION

Technical Report 32-1447

Laminar Flow Heat Transfer From a Gaseous Plasma at Elevated Electron Temperature in the Presence of Electromagnetic Fields

T. K. Bose

JET PROPULSION LABORATORY
CALIFORNIA INSTITUTE OF TECHNOLOGY
PASADENA, CALIFORNIA

March 1, 1970

NATIONAL AERONAUTICS AND SPACE ADMINISTRATION

Technical Report 32-1447

Laminar Flow Heat Transfer From a Gaseous Plasma at Elevated Electron Temperature in the Presence of Electromagnetic Fields

T. K. Bose

JET PROPULSION LABORATORY
CALIFORNIA INSTITUTE OF TECHNOLOGY
PASADENA, CALIFORNIA

March 1, 1970

Prepared Under Contract No. NAS 7-100
National Aeronautics and Space Administration

Preface

The work described in this report was performed by the Propulsion Division of the Jet Propulsion Laboratory.

Acknowledgment

The author wishes to thank the National Aeronautics and Space Administration and the National Research Council for financial support in the form of a NASA–NRC Resident Research Associateship.

Contents

Contents (contd)

Figures

Abstract

A comparatively general theoretical analysis is presented for a laminar steady flow of an ionized gas in the continuum region, with emphasis placed on the heat transfer. The effects of applied electromagnetic fields, nonequilibrium temperature and composition, and variable thermophysical properties are taken into account. A two-temperature plasma is considered in which the electron temperature may exceed the temperature of the heavy particles.

Laminar Flow Heat Transfer From a Gaseous Plasma at Elevated Electron Temperature in the Presence of Electromagnetic Fields

I. Introduction

Electrode erosion in plasma-propulsion and power-generation devices can be caused by intense heat flux to the electrodes, especially at the anode. In the past, theoretical evaluation of anode heat flux was severely limited; only heat flux from a high-temperature gaseous plasma without an electromagnetic field could be predicted. Most of the earlier work relating to plasmas was confined to reentry problems. Experiments were conducted by Gruszczynski (Ref. 1) and Rose (Ref. 2) in which heat-transfer data at the stagnation point were obtained for axisymmetric bodies in shock tubes. It was found that $Nu/(Re)^{1/2}$ was almost independent of the flight velocity. Park (Refs. 3 and 4) measured the heat transfer in an argon-arc tunnel, and his results indicated that this was true for the frozen condition. Theoretical investigations of the different aspects of heat transfer from laminar boundary layers were made by several authors. Bade (Ref. 5) solved the stagnation-point boundary-layer equations by introducing a power series in the viscosity coefficient. Similar approaches were also taken by Back (Refs. 6 and 7) and Mirels (Refs. 8 and 9). Bose (Ref. 10) solved several different cases of plasma heat transfer, including the boundary layer, which were numerically exact for the nitrogen and argon plasmas in the equilibrium condition. The thermophysical-properties data were taken from Penski (Ref. 11) and others (Refs. 12 and 13). Bose found that $Nu(\rho_\infty/\rho_w)/(Re)^{1/2}$ can become as large as half the value it has for a low-temperature gas for which properties are assumed to be constant.

An important breakthrough in predicting the heat transfer from a two-temperature plasma was achieved by devising methods to compute the composition of two-temperature gases (Refs. 14–16) and by introducing terms due to enthalpy transport by electrons (Refs. 17 and 18). Shih and associates (Refs. 19 and 20) presented a simple anode heat-transfer model. The contribution of the electric current to the anode heat flux is separated from other heat-transfer mechanisms in this model; the overall contribution of the electric current to the anode heat flux is expressed as the sum of individual contributions from the anode fall, the work function of the anode material, and the enthalpy carried by the electron current. Another important contribution to the understanding

of a two-temperature boundary layer is an analysis of magnetohydrodynamics (MHD) channel flow made by Sherman and Reshotko (Ref. 21). They presented for the first time an analysis of the boundary layer of a two-temperature fluid for which applied electromagnetic fields, current flow, and the presence of a sheath are taken into account.

The basic difference between the analyses of all of the references cited and the present analysis is that the former pertain to boundary-layer flows only, whereas the present analysis is more general. It does not include the boundary-layer restrictions, except where such restrictions may be imposed as a special case.

Some comments on signs pertaining to the present analysis should be noted. The electron charge is assumed to be positive (e^+). This means that the motion of the electrons in a positive coordinate direction produces a positive current density. Although this is not the established convention, it has been found to be very useful because the electrons and not the ions are mainly responsible for the current flow.

II. Fundamental Equations

The following quantities are assumed to be known: (1) the electron and heavy-particle temperatures T_e and T_h, respectively, at a reference point; (2) the pressure p; (3) the gas velocity $\mathbf{V}$; (4) the kind of gas; (5) the characteristic length L of the model; and (6) the magnitude of any externally applied electromagnetic fields. Furthermore, the analysis is based on a physical model in which the following apply: (1) The gravitational effects are neglected. (2) The radiation pressure is small. (3) The Hall parameter is small, and hence the thermophysical properties are independent of directions. (4) The current is carried mainly by electrons; therefore, $\mathbf{j}_i = 0$ and $\mathbf{j} = +\mathbf{j}_e$. (5) A quasineutral plasma exists; that is, $n_e = \Sigma\ i \times n_i$, where i is the degree of ionization. (6) The plasma consists only of atoms, electrons, and singly charged ions.

A few remarks are in order concerning the physical model. It is known that, in an electric field, the electrons move much faster than do the ions. For example, considering a typical case of an argon plasma at 1 atm in an electric field of 100 V/m, the characteristic drift or field velocity for electrons is 600 m/s; for ions, it is 1 m/s. To maintain quasineutrality, the electron flux in a field must be constant; that is, $\nabla \cdot \dot{\mathbf{n}}_{ef} = 0$, which also means that $\nabla \cdot \mathbf{j} = 0$. In addition to the fact that electrons move fast in the electric field, they may also diffuse in pairs with the ions (Fig. 1). That is, independent of the externally applied electric field, electrons and ions move in pairs at a diffusive velocity consistent with the ambipolar diffusion coefficient D_{amb} (Refs. 22 and 23) given by the relation

$$D_{amb} = \frac{2\,D_{ea}\,D_{ei}}{(D_{ea} + D_{ei})} \tag{1}$$

In addition to these two velocities, designated as the field and diffusive velocities, a third is the directed-mass average velocity of the particles.

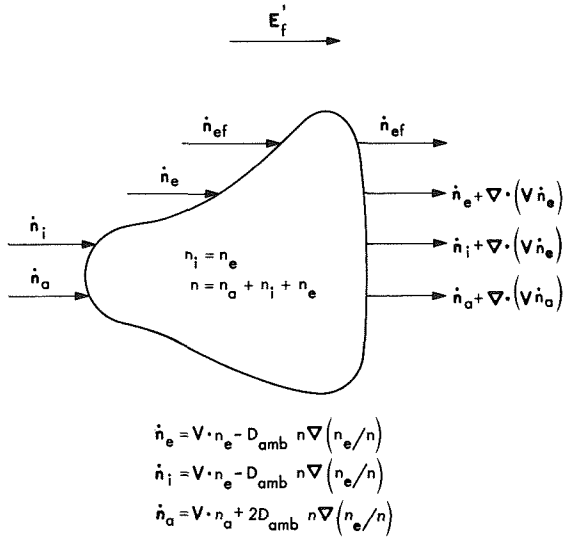

Fig. 1. Flux of particles $\dot{n}$

For a steady-state condition, in the absence of any externally applied field, the diffusion flux of atoms must be equal to the sum of the diffusion fluxes of the electrons and ions. Thus, atoms also diffuse at a drift velocity consistent with the diffusion coefficient D_{amb}.

The paragraphs that follow contain the relevant equations.

A. Equations of State

For a two-temperature plasma, the equation of state is

$$p = k_B \left(T_e n_e + T_h \sum_h n_j \right), \text{ bar} \tag{2}$$

Since $\rho_j = k_B\, m_j\, n_j/R^*$, and $\theta_j = T_e/T_h$, Eq. (2) can also be rewritten as

$$p = \frac{R^*\, T_h\left[\theta\left(\frac{m_h}{m_e}\right)\rho_e + \sum_h \rho_i\right]}{m_h}, \text{ bar} \tag{3}$$

B. Equation of Continuity of Species

In terms of number density, the equation for continuity of the jth species is

$$\nabla \cdot (n_j \mathbf{V}_j) = R_j, \text{ m}^{-3}\text{ s}^{-1} \tag{4}$$

where R_j is the number rate of production of the jth species by chemical reaction. Now,

$$\mathbf{V}_j = \mathbf{V} + \mathbf{V}'_{\text{dj}} + \mathbf{V}'_{\text{fj}} \tag{5}$$

where $\mathbf{V}$ is the directed-mass averaged velocity, $\mathbf{V}'_{\text{dj}}$ is the diffusive velocity of species caused by the concentration gradient, and $\mathbf{V}'_{\text{fj}}$ is the field velocity of the species in an electromagnetic field given by the relation

$$\mathbf{V}'_{\text{fj}} = \mu_j \mathbf{E}_f = \frac{\mathbf{j}_j}{e_j n_j} = \frac{\mathbf{j}_j}{\rho_{\text{el,j}}} \tag{6}$$

This gives two different definitions of current; namely, the convection current,

$$\mathbf{j}_{\text{cj}} = e_j n_j \mathbf{V}_j \tag{7}$$

which is the total charge carried by the jth species per unit area and time, and the field current,

$$\mathbf{j}_j = e_j n_j \mathbf{V}'_{\text{fj}} \tag{8}$$

which is a portion of the convection current.

By multiplying Eq. (4) by $k_B m_j/R^*$, and taking the continuity of current into account, one can rewrite Eq. (4) in a much simpler form. Since

$$\rho_j \mathbf{V}'_{\text{dj}} = -\rho\, D_{\text{amb}}\, \nabla\, g_j \tag{9a}$$

$$g_j = \frac{\rho_j}{\rho} \tag{9b}$$

Equation (4) becomes

$$\nabla \cdot (\rho_j \mathbf{V}) - \nabla \cdot (\rho\, D_{\text{amb}}\, \nabla\, g_j) = m_{\text{Rj}}, \text{kg/m}^3\text{-s} \tag{10}$$

The quantity m_{Rj} is the mass rate of production of the species.

C. Equation of Global Continuity

If Eq. (10) is added over all species, and it is noted that $\rho = \Sigma\rho_i$, and that $\Sigma m_{\text{Rj}} = 0$, the global-continuity equation is

$$\nabla \cdot (\rho \mathbf{V}) = 0 \tag{11}$$

D. Equation of Motion of Species

For the jth species,

$$\nabla \cdot (\rho_j \mathbf{V}^r_j\, \mathbf{V}^s_j) = \nabla \cdot \boldsymbol{\tau}^{\text{rs}}_j + \mathbf{F}^r_{\text{jf}} \tag{12}$$

where

$$\boldsymbol{\tau}^{\text{rs}}_j = \left(-p_j - \frac{2}{3}\eta_j \nabla \cdot \mathbf{V}_j\right)\delta^{\text{rs}} + \eta_j\, \boldsymbol{\omega}^{\text{rs}}_j$$

$$\delta^{\text{rs}} = \text{Kronek's delta: } \delta^{\text{rs}} = 0,\ \delta^{\text{rr}} = 1 \tag{13}$$

$$\boldsymbol{\omega}^{\text{rs}}_j = \frac{\partial \mathbf{V}^r_j}{\partial x^s} + \frac{\partial \mathbf{V}^s_j}{\partial x^r}$$

and

$$\mathbf{F}^r_{\text{jf}} = n_j e_j (\mathbf{E}'_f + \mathbf{V}_j \times \mathbf{B}) = \rho_{\text{el,j}} (\mathbf{E}'_f + \mathbf{V}_j \times \mathbf{B})$$

E. Equation of Global Motion

If Eq. (12) is added over all species, the equation of global motion becomes

$$\rho(\mathbf{V}^r \nabla) \cdot \mathbf{V}^s = \nabla \cdot \boldsymbol{\tau}^{\text{rs}} + \mathbf{j} \times \mathbf{B} \tag{14}$$

where

$$\boldsymbol{\tau}^{\text{rs}} = \left(-p - \frac{2}{3}\eta\, \nabla \cdot \mathbf{V}\right)\delta^{\text{rs}} + \eta \boldsymbol{\omega}^{\text{rs}}$$

$$\delta^{\text{rs}} = 0, \qquad \delta^{\text{rr}} = 1$$

$$\boldsymbol{\omega}^{\text{rs}} = \frac{\partial \mathbf{V}^r}{\partial x^s} + \frac{\partial \mathbf{V}^s}{\partial x^r} \tag{15}$$

$$\mathbf{j} = \Sigma\rho_{\text{el,j}}\, \mathbf{V}'_{\text{fj}} = \Sigma \mathbf{j}_j$$

F. Equation of Energy of Species

For the jth species, the energy equation is

$$\nabla \cdot (\rho_j \mathbf{V}_j E^o_j) = \nabla \cdot (k_j\, \nabla\, T_j) + \nabla \cdot (\mathbf{V}_j\, \boldsymbol{\tau}^{\text{rs}}_j) + Q_{\text{jf}} + Q_{\text{jc}} - \Sigma_{\text{Rj}} \tag{16}$$

where

$$E_j^o = E_j + \frac{|\mathbf{V}_j^2|}{2} = \frac{3}{2}\frac{R^*}{m_j}T_j + I_{\mathrm{mj}} + \frac{|\mathbf{V}_j^2|}{2}$$

Q_{jc} = energy transferred by molecular encounter (elastic + inelastic) = $Q_{\mathrm{j,coll}} + Q_{\mathrm{j,chem}}$

$$Q_{\mathrm{jf}} = \mathbf{V}'_{\mathrm{fj}}\ \rho_{\mathrm{el,j}}(\mathbf{E}'_f + \mathbf{V}_j \times \mathbf{B}) = \mathbf{j}_j \cdot \mathbf{E}'_f$$

Now,

$$\begin{aligned}\nabla\cdot(\rho_j\mathbf{V}_jE_j^o) &= \nabla\cdot(\rho_j\mathbf{V}_jE_j) + \sum_r \mathbf{V}_j^r\,\nabla\cdot(\rho_j\mathbf{V}_j^r\mathbf{V}_j^s)\\ &\quad + |\mathbf{V}_j^2|\,\nabla\cdot\frac{(\rho_j\mathbf{V}_j)}{2}\\ &= \nabla\cdot(\rho_j\mathbf{V}E_j) + \nabla\cdot(\rho_j\mathbf{V}'_{\mathrm{dj}}E_j)\\ &\quad + \nabla\cdot(\rho_j\mathbf{V}'_{\mathrm{fj}}E_j)\\ &\quad + \sum_r \mathbf{V}_j^r\,\nabla\cdot(\rho_j\mathbf{V}_j^r\mathbf{V}_j^s)\\ &\quad + \frac{|\mathbf{V}_j^2|}{2}m_{\mathrm{Rj}}\end{aligned} \tag{17}$$

Also,

$$\begin{aligned}\nabla\cdot(\rho_j\mathbf{V}E_j) &= \frac{3}{2}\frac{R^*}{m_j}\rho\mathbf{V}\,\nabla\cdot(g_jT_j) + \rho\mathbf{V}\,\nabla\cdot(g_j\mathbf{V}_j^2)\\ &\quad + \rho\mathbf{V}\,\mathbf{I}_{\mathrm{mj}}\,\nabla\cdot g_j\end{aligned} \tag{18}$$

If Eqs. (17) and (18) are substituted into Eq. (16), and it is noted that $g_i + g_a = 1$ and $\mathbf{V}_i \approx \mathbf{V}_a \approx \mathbf{V}$, the two energy equations for the electrons and heavy particles are as given below.

For the electrons:

$$\begin{aligned}\frac{3}{2}\frac{R^*}{m_e}\rho\mathbf{V}\,\nabla\cdot(g_eT_e) &= \frac{3}{2}\frac{R^*}{m_e}\nabla\cdot(\rho D_{\mathrm{amb}}T_e\,\nabla g_e)\\ &\quad + \nabla\cdot(k_e\,\nabla T_e) - \frac{3}{2}\frac{k_B}{e}\nabla\cdot(\mathbf{j}T_e)\\ &\quad + \mathbf{j}\cdot\mathbf{E}'_f + Q_{\mathrm{e,chem}}\\ &\quad - \frac{3m_e}{m_h}k_B(T_e - T_h)\Gamma_{\mathrm{eh}},\ \mathrm{J/m^3\text{-}s}\end{aligned} \tag{19}$$

For the heavy particles:

$$\begin{aligned}\frac{3}{2}\frac{R^*}{m_h}\rho\mathbf{V}\,\nabla\cdot T_h + \rho\mathbf{V}\,\nabla\cdot\mathbf{V}^2 + \rho\mathbf{V}I_{\mathrm{mi}}\,\nabla g_i &=\\ \nabla\cdot(\rho D_{\mathrm{amb}}I_{\mathrm{mi}}\,\nabla g_i)&\\ + \nabla\cdot(k_h\,\nabla T_h + \frac{3m_e}{m_h}k_B(T_e - T_h)\Gamma_{\mathrm{eh}}&\\ - Q_{\mathrm{e,chem}} + \nabla\cdot(\mathbf{V}\boldsymbol{\tau}^{\mathrm{rs}})&\end{aligned} \tag{20}$$

G. Equation of Global Energy

If Eq. (16) is added over all species, and it is noted that

$$\begin{aligned}\sum\nabla\cdot(\rho_j\mathbf{V}_jE_j^o) &= \nabla\cdot(\rho E^o\mathbf{V}) + \nabla\cdot\sum\rho_j\mathbf{V}'_jE_j\\ \sum\nabla\cdot(\mathbf{V}_j\boldsymbol{\tau}_j^{\mathrm{rs}}) &= \nabla\cdot(\mathbf{V}\boldsymbol{\tau}^{\mathrm{rs}}) - \nabla\cdot\sum(p_j\mathbf{V}'_j)\end{aligned} \tag{21}$$

the following equation is obtained:

$$\begin{aligned}\nabla\cdot(\rho E^o\mathbf{V}) &= \sum\nabla\cdot(k_j\,\nabla T_j) - \sum\nabla\cdot[\rho_j\mathbf{V}'_j(E_j + p_j/\rho_j)]\\ &\quad + \nabla\cdot(\mathbf{V}\boldsymbol{\tau}^{\mathrm{rs}}) + \mathbf{j}\cdot\mathbf{E}'_f - \sum\epsilon_{\mathrm{Rj}}\end{aligned} \tag{22}$$

Now, if it is noted that

$$\sum\epsilon_{\mathrm{Rj}} = \epsilon_R,$$

$$\begin{aligned}\sum\nabla\cdot[\rho_j\mathbf{V}'_j(E_j + p_j/\rho_j)] &= -\nabla\cdot\rho D_{\mathrm{amb}}I_{\mathrm{mi}}\,\nabla g_i\\ &\quad - \nabla\cdot\rho D_{\mathrm{amb}}\frac{5}{2}\frac{R^*}{m_e}T_e\nabla g_e\\ &\quad + \frac{5}{2}\frac{k_B}{e}\nabla\cdot(\mathbf{j}T_e)\end{aligned} \tag{23}$$

Equation (22) becomes

$$\begin{aligned}\rho\mathbf{V}\nabla\cdot E^o &= \nabla\cdot\sum k_j\,\nabla T_j + \nabla\cdot(\rho D_{\mathrm{amb}}I_{\mathrm{mi}}\,\nabla g_i)\\ &\quad + \frac{5}{2}\frac{R^*}{m_e}\nabla\cdot(\rho D_{\mathrm{amb}}T_e\,\nabla g_e)\\ &\quad - \frac{5}{2}\frac{k_B}{e}\nabla\cdot(jT_e) + \nabla\cdot(\mathbf{V}\boldsymbol{\tau}^{\mathrm{rs}}) + j\cdot E'_f - \epsilon_R\end{aligned} \tag{24}$$

If the global-momentum equation is multiplied by $\mathbf{V}^r$ for respective directions, and these are added, the equation for kinetic energy is obtained. By subtracting this from Eq. (24), is may be shown (after some transformation) that

$$\rho\mathbf{V}\nabla\cdot h - \mathbf{V}\nabla\cdot p = \nabla\cdot(k_h\,\nabla T_h) + \nabla\cdot(k_e\,\nabla T_e) + \nabla\cdot(\rho D_{\mathrm{amb}} I_{\mathrm{mi}}\,\nabla g_i) + \frac{5}{2}\frac{R^*}{m_e}\nabla\cdot(\rho D_{\mathrm{amb}} T_e\,\nabla g_e) - \frac{5}{2}\frac{k_B}{e}\nabla\cdot(\mathbf{j}T_e) + \frac{|\mathbf{j}^2|}{\sigma} + \phi \tag{25}$$

where

$$\phi = (\boldsymbol{\tau}^{\mathrm{rs}} + p)\,\nabla\cdot\mathbf{V}\ (\text{the dissipation function}) \tag{26}$$

and

$$h = \frac{5}{2}\frac{R^*}{m_h}T_h + \frac{5}{2}\frac{R^*}{m_e}T_e\,g_e + I_{\mathrm{mi}}\,g_i \tag{27}$$

H. Electromagnetic Equations

For a steady-state condition and a quasineutral plasma, Maxwell's equations are

$$\nabla\times\mathbf{E}'_f = 0, \qquad \nabla\cdot\mathbf{E}'_f = 0$$
$$\nabla\times\mathbf{H} = \mathbf{j}, \qquad \nabla\cdot\mathbf{B} = 0 \tag{28}$$

and Ohm's law is

$$\mathbf{j} = \sigma\,[\mathbf{E}'_f + (\mathbf{V}\times\mathbf{B})] + \frac{1}{en_e}\nabla\,p_e - \frac{1}{en_e}(\mathbf{j}\times\mathbf{B}) \tag{29}$$

III. Heat Transfer

A. General Heat-Transfer Relations at the Wall

Validity of the continuum theory is assumed in the main flow field to a location b, which is a mean free path of the collected particles from the surface (Fig. 2). This mean free path is much longer than the distance across which the applied electric potential on the surface is shielded (sheath region). At moderate pressures ($p > 1$ atm), it is found that the electron mean free path λ_e is much longer than the Debye shielding distance λ_D, whereas the ion mean free path $\lambda_i \simeq \lambda_D$ (Ref. 24).

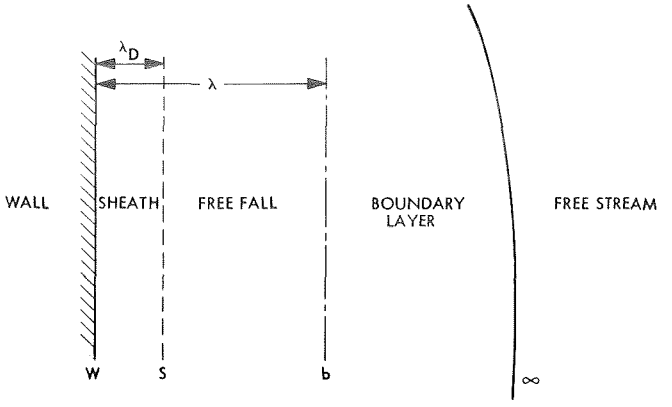

Fig. 2. Different regions near the wall

The heat flux at the wall is the convective heat flux at b plus the energy gained (or lost) in the free-fall region and the radiative heat flux to the surface:

$$\mathbf{q}_w = \mathbf{q}_b - \Delta q + \mathbf{q}_R \tag{30}$$

It should be noted that heat added to the gas (including energy transfer to the particles being accelerated in the sheath) is considered to be positive. Thus, heat transferred to the wall is negative. From Eq. (25), the convective heat flux at the edge of the sheath, which is transferred to the wall, is

$$\boldsymbol{q}_b = -k_h\,\nabla T_h - k_e\,\nabla T_e - \rho D_{\mathrm{amb}} I_{\mathrm{mi}}\,\nabla g_i - \frac{5}{2}\frac{R^*}{m_e}\rho D_{\mathrm{amb}} T_e\,\nabla g_e + \frac{5}{2}\frac{k_B}{e}\mathbf{j}\,T_{eb} \tag{31}$$

The gradients and properties in Eq. (31) are evaluated at b (see Fig. 2). It is to be noted that k_h and k_e are not the heat-conductivity coefficients of the "pure" gases, but specify only the contribution from the heavy particles and electrons. With the help of Fay's mixing rule (Ref. 25), it can be shown that k_e is of the order $(x_e k'_e)$, and that k_h is of the order $(x_a k'_a + x_i k'_i)$; where $x_j = n_j/n$, the mol ratio and primes denote the heat-conductivity coefficient of "pure" gases.

For many cases, the mol fraction of electrons x_e at the wall is very small. In addition, for a quasineutral plasma, $g_i = m_h\ g_e/m_e$. Equation (31), therefore,

reduces to

$$\mathbf{q}_b = -k_h \nabla T_h - \rho D_{\text{amb}} \left(I_{\text{mi}} \frac{m_h}{m_e} + \frac{5}{2} \frac{R^*}{m_e} T_e \right) \nabla g_e + \frac{5}{2} \frac{k_B}{e} \mathbf{j} T_{\text{eb}} \tag{32}$$

In some instances, it is useful to define an effective heat-conductivity coefficient by the relation

$$k = k_h + \rho D_{\text{amb}} \left(I_{\text{mi}} \frac{m_h}{m_e} + \frac{5}{2} \frac{R^*}{m_e} T_e \right) \frac{dg_e}{dT_h} + k_e \frac{dT_e}{dT_h} \tag{33}$$

Equation (33) has unique solutions for frozen and equilibrium plasmas. The effective heat flux to the wall is given by the relation

$$\mathbf{q}_w = -k_h \nabla T_h + \frac{5}{2} \frac{k_B}{e} \mathbf{j} T_{\text{eb}} - \Delta q + \mathbf{q}_R \tag{34}$$

B. Sheath Analysis

1. Species in a decelerating field. To compute the energy gain (or loss) in the sheath Δq, a potential φ_w is applied to the body surface to retard the jth species and to attract the kth species. The jth species reaches the wall in free fall provided that the random velocity at b is $v_j \geq (2e \mid \varphi_w \mid /M_j)^{1/2}$. The flux of the jth species reaching the wall n_{jw} and their associated energy flux at b is, therefore, found by integrating from $(2e \mid \varphi_w \mid /M_j)^{1/2}$ to infinity and not zero to infinity (Ref. 26). Thus,

$$\dot{\mathbf{n}}_{\text{jw}} = -\dot{n}_{\text{jb}} \left(\frac{k_B T_j}{2\pi M_j} \right)^{1/2} \exp \left(\frac{-e \mid \varphi_w \mid}{k_B T_j} \right), \text{ m}^{-2}\,\text{s}^{-1} \tag{35}$$

$$\mathbf{q}_{\text{jb}} = -n_{\text{jb}} \left(\frac{k_B T_j}{2\pi M_j} \right)^{1/2} (e \mid \varphi_w \mid + 2 k_B T_j) \exp \left(\frac{-e \mid \varphi_w \mid}{k_B T_j} \right) = \dot{\mathbf{n}}_{\text{jw}} (e \mid \varphi_w \mid + 2 k_B T_j), \text{ J/m}^2\text{-s} \tag{36}$$

The loss of energy in the retarding field is $\Delta \mathbf{q}_j = -\dot{\mathbf{n}}_{\text{jw}} e \mid \varphi_w \mid$; therefore, the net energy flux from the jth species to the wall is

$$q_{\text{jw}} = 2 \dot{\mathbf{n}}_{\text{jw}} k_B T_j, \text{ J/m}^2\text{-s} \tag{37}$$

2. Species in an accelerating field. Similarly, for the accelerating kth species, the flux of particles at the wall, as well as the associated energy fluxes at b and w and the gain, are

$$\dot{\mathbf{n}}_{\text{kb}} = \dot{\mathbf{n}}_{\text{kw}} = -n_{\text{kb}} \left(\frac{k_B T_k}{2\pi M_k} \right)^{1/2} \tag{38a}$$

$$\mathbf{q}_{\text{kb}} = -n_{\text{kb}} \left(\frac{k_B T_k}{2\pi M_k} \right)^{1/2} (2 k_B T_k) = 2 k_B T_k \dot{\mathbf{n}}_{\text{kw}} \tag{38b}$$

$$\mathbf{q}_{\text{kw}} = \dot{\mathbf{n}}_{\text{kw}} (2 k_B T_k + e \mid \varphi_w \mid) \tag{38c}$$

$$\Delta q_k = \dot{\mathbf{n}}_{\text{kw}} e \mid \varphi_w \mid \tag{38d}$$

3. Species emitted from the wall. In the case of a mass flux of jth species being emitted from the wall, namely, $\dot{\mathbf{n}}'_{\text{jw}}$, there is an associated energy flux at the wall:

$$\mathbf{q}'_{\text{jw}} = \Delta q'_j = \dot{\mathbf{n}}_{\text{jw}} (E_{\text{jw}} + e \phi_w) \tag{39}$$

where E_j is the average energy of the particles just emitted and ϕ_w is the work function of the material. The process may also be considered in another way. The free electrons, when they "condense" on the wall, give rise to a heat flux that is expressed as

$$\mathbf{q}'_{\text{ew}} = \Delta q'_e = \dot{\mathbf{n}}_{\text{ew}} e \phi_w = \mathbf{j}_e \phi_w \tag{40}$$

4. Recombination at the wall. Furthermore, there is also a possibility that a flux of the jth species $\dot{\mathbf{n}}_{\text{jw}}$ recombine with their counterparts at the wall, and release an energy:

$$\mathbf{q}''_{\text{jw}} = \Delta q''_j = \dot{\mathbf{n}}''_{\text{jw}} (I_j - e \phi_w) \tag{41}$$

Several special physical cases for which evaluation of the heat flux to the wall is considered are discussed below.

C. Heat Transfer at the Anode

At the anode, the current is carried mainly by the accelerating electrons:

$$\mathbf{j} = e\, n_{\text{eb}} \left(\frac{k_B T_{\text{eb}}}{2\pi M_e} \right)^{1/2} \tag{42}$$

Thus, the equation for the total heat flux from Eqs. (34), (38), and (40) becomes

$$\mathbf{q}_A = \mathbf{q}_b - \mathbf{j} (\varphi_A + \phi_w) + \mathbf{q}_R = -k (\nabla T_h)_b + \frac{5}{2} \frac{k_B}{e} \mathbf{j} T_{\text{eb}} - \mathbf{j} (\varphi_A + \phi_w) + \mathbf{q}_R \tag{43}$$

Equation (43) is the same as Eqs. (83) and (89) of Eckert and Pfender (see Ref. 19).

D. Heat Transfer at the Cathode

Generally, the ion current attracted at the cathode is very small and the current is maintained by thermionic or field emissions from the surface (Ref. 27). A simple estimation of the different emission mechanisms shows clearly that thermionic emission is indeed the dominating mechanism in high-intensity arcs. For such cases (neglecting the enthalpy of the emitted electrons), the total heat flux to the wall is

$$\mathbf{q}_c = \mathbf{q}_b - \mathbf{j}\,\phi_w \simeq -k\,(\nabla\, T_h)_b + \frac{5}{2}\,\frac{k_B}{e}\,\mathbf{j}\,T_{\mathrm{eb}} - \mathbf{j}\,\phi_w + \mathbf{q}_R \tag{44}$$

E. Heat Transfer to an Insulated Conducting Wall Between the Electrodes

A conducting wall placed between the electrodes, but insulated from them (Fig. 3), is capable of circulating an electric current. Near the cathode, the wall is positive with respect to the plasma, and the electrons may flow to the wall. Near the anode, the wall is negative with respect to the plasma, and the ions may drift to the wall and recombine, thus giving rise to an effective current $\mathbf{j}$ flowing through the wall. The heat flux to the wall in this case is

$$\begin{aligned}\mathbf{q}_w &= \mathbf{q}_b - \dot{\mathbf{n}}_{\mathrm{ew}}\, e\,\phi_w + \dot{\mathbf{n}}_{\mathrm{iw}}\,(I_i - e\,\phi_w) + \mathbf{q}_R \\ &= \mathbf{q}_b + \frac{\mathbf{j}}{e}\,I_i + \mathbf{q}_R = -k\,(\nabla\, T_h)_b \\ &\quad + \frac{5}{2}\,\frac{k_B}{e}\,\mathbf{j}\,T_{\mathrm{eb}} + \frac{\mathbf{j}}{e}\,I_i + \mathbf{q}_R \end{aligned} \tag{45}$$

where I_i is the ionization energy of the ions in electron-volts. Unfortunately, it is difficult to estimate the current. For segmented or nonconducting walls, $\mathbf{j} = 0$, and Eq. (45) reduces to the usual heat-transfer relation for a plasma in which there is no current flow.

F. Electrostatic Probes

Electrostatic probes are very simple instruments that may be used to measure the electron temperature of the free electrons of a gaseous plasma. Detailed theory and experiments are contained in the excellent review by Cheng (Ref. 28). Such probes are cooled, and are characterized by no surface emission. The current density is

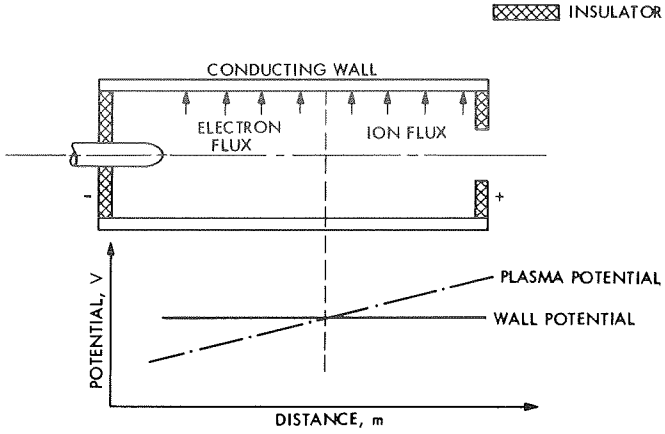

Fig. 3. Current flow and potential in a conducting wall between two electrodes

of the order of magnitude of 0.1 A/mm^2. The probe is both positively and negatively biased with respect to the plasma; for a strongly negative probe, the current is carried mainly by the ions recombining on the surface. The cases to be distinguished are described in the paragraphs that follow.

1. Slightly negative or strongly positive probe. If it is assumed that the potential applied to the probe is effectively shielded in a region of thickness within an order of magnitude of a Debye shielding distance, the current flowing to the probe (see Ref. 24) is

$$\begin{aligned}\mathbf{j} &= -e\,n_{\mathrm{eb}}\left(\frac{k_B\,T_{\mathrm{eb}}}{2\pi\,M_e}\right)^{1/2}\epsilon \\ &= -e\,D_{\mathrm{amb}}\,\nabla\, n_{\mathrm{eb}}\end{aligned} \tag{46}$$

where

$$\begin{aligned}\epsilon &= \exp\left(\frac{e\,\varphi_w}{k\,T_e}\right), \qquad \varphi_w \leq 0 \\ &= 1, \qquad \varphi_w \geq 0\end{aligned} \tag{47}$$

From Eqs. (2), (3), and (46), the boundary condition at b is

$$g_{\mathrm{eb}}\left(\frac{k_b\,T_{\mathrm{eb}}}{2\pi\,M_e}\right)^{1/2}\epsilon = D_{\mathrm{amb}}\,(\nabla\, g_e)_b \tag{48}$$

where

$$g_e = \frac{\rho_e}{\rho} \tag{49a}$$

and

$$\rho_e = \left(\frac{k_B m_e}{R^*}\right) n_e \tag{49b}$$

The current density, computed from Eqs. (48) and (46) for a given applied probe potential, is substituted into the anode heat-transfer relation (Eq. 43) to compute the heat flux.

2. Strongly negative probes. If it is assumed that the potential applied to the probe is effectively shielded within the free-fall region of ions, $n_{eb} = n_{ib}$, and the current is

$$\mathbf{j} = e\, n_{eb}\left(\frac{k_B T_{hb}}{2\pi M_h}\right)^{1/2} \tag{50}$$

The boundary condition for the electrons is

$$(\nabla\, g_e)_b = 0 \tag{51}$$

The heat flux to the probe by recombination is

$$\mathbf{q}_w = -k\,(\nabla\, T_h)_b + \frac{\mathbf{j}}{e}\,(I_i - e\,\phi_w) + \mathbf{q}_R \tag{52}$$

IV. Similarity Laws

A parametric study of the differential equations is now made to determine the importance of different dimensionless numbers. As a first approximation, the following assumptions are believed to be justified:

(1) The induced magnetic field is small and the applied magnetic field does not substantially change the pressure.

(2) The thermophysical properties are represented by their average values.

(3) The plasma is either considered as frozen or in thermodynamic equilibrium, except that $T_e \neq T_h$.

(4) The radiation is neglected.

(5) The compression and viscous terms in the energy equation are neglected.

(6) The electron pressure and Hall effects are neglected.

As a consequence, the fundamental equations are:

Continuity:

$$\nabla \cdot \mathbf{V} = 0 \tag{53}$$

Motion:

$$\rho\,(\mathbf{V}\,\nabla\,)\cdot\mathbf{V} = -\nabla\, p + \eta\,\nabla^2\mathbf{V} + \mathbf{j}\times\mathbf{B} \tag{54}$$

Energy:

$$\rho\,\mathbf{V}\,\nabla\cdot h \approx \rho\,\mathbf{V}\,c_p\,\nabla\cdot T_h = -\nabla\cdot\mathbf{q} + \frac{|j^2|}{\sigma}$$
$$\mathbf{q} = -k\,\nabla\,T_h + \frac{5}{2}\,\frac{k_B}{e}\,\mathbf{j}\,T_e \tag{55}$$

Heat flux at b:

$$\mathbf{q}_b = -k\,\nabla\,T_h + \frac{5}{2}\,\frac{k_B}{e}\,\mathbf{j}\,T_{eb} = \alpha\,\Delta\,T_h \tag{56}$$

Equations (53) through (56) lead to the following heat-transfer relation:

$$Nu = Nu\,(Re, Pr, \theta, N_1, N_2, N_3) \tag{57}$$

where

$$Nu = \frac{\alpha L}{k}, \qquad L = \text{a characteristic length}$$
$$Re = \frac{\rho U L}{\eta}, \qquad Pr = \frac{\eta\, cp}{k}$$
$$\theta = \frac{T_e}{T_h}$$
$$N_1 = \frac{|j|\,BL}{(\rho U^2)}, \qquad U = \text{a characteristic velocity}$$
$$N_2 = \frac{|j^2|\,L}{\sigma\,\rho\,\mathrm{U}\,cp\,\Delta\,T_h}$$
$$N_3 = \frac{5\,k_B\,|j|\,L}{2\,k\,e} \tag{58}$$

The three dimensionless parameters N_1, N_2, and N_3 have the following meanings: N_1 is the ratio of the Lorentz force to the dynamic pressure; N_2 is the ratio of the production of heat by joule heating to the convection of heat; and N_3 represents the ratio of enthalpy transport by the electrons to the heat conduction.

For no current flow ($j = 0$), Eq. (57) reduces to

$$Nu = Nu\,(Re, Pr, \theta) \tag{59}$$

Only for $\theta = 1$ is it possible to use all low-temperature heat-transfer relations suitably modified to account for variable properties.

V. Flow Between Two Parallel Flat Plates

The effect of current on heat transfer will be better understood if a simplified problem is now considered. A conducting fluid is assumed to flow in a channel between two parallel flat plates, as shown in Fig. 4. In addition, it is assumed that a uniform current **j** is flowing between the cathode c and the anode A, that the temperature and velocity profiles are fully developed, and that the thermophysical properties are constant. The assumption of constant thermophysical properties is not correct for a pure gas plasma, but is reasonably realistic for seeded plasmas. It is also assumed that $T = T_e = T_h$ in the continuum region. The temperatures at the two edges of the sheath are assumed to be the same as the two temperatures at the walls. Electrons are moving readily from the wall to the fluid, and vice versa, with the work function zero ($\phi_w = 0$). For cold walls with very little thermionic emission, the small work function allows the electrons to move freely without excessive potential drop near the cathode. The electric field near both walls will be the same as the average applied field $\mathbf{E}_{\text{appl}} = \mathbf{j}/\sigma$.

The solution of the continuity and momentum equations with no slip condition at the sheath edge gives essentially the solution of a Hagen–Poiseuille flow. The energy and heat-flux equations at the sheath edge (boundary b) are:

Energy:

$$k\frac{d^2T}{dy^2} = -\frac{|j^2|}{\sigma} + \frac{5}{2}\frac{k_B}{e}\mathbf{j}\frac{dT}{dy} \tag{60}$$

Heat flux at b:

$$q_b = -k\frac{dT}{dy} + \frac{5}{2}\frac{k_B}{e}\mathbf{j}\,T \equiv -\alpha\,(T_A - T_c) \tag{61}$$

The variable α is the convective heat-transfer coefficient, T_A is the anode surface temperature, and T_c is the cathode surface temperature.

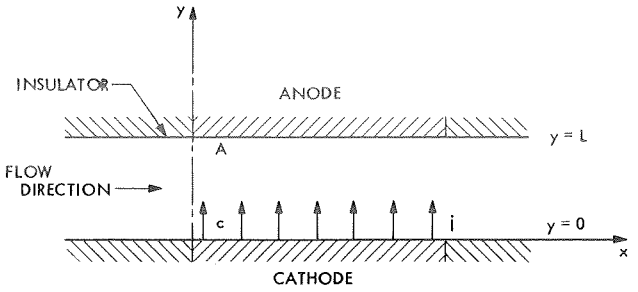

Fig. 4. Current flow between two parallel plates

With $T^* = T/T_c$ and $y^* = y/L$, Eqs. (60) and (61) are nondimensionalized into

$$\frac{d^2T^*}{dy^{*2}} = N_3\frac{dT^*}{dy^*} - N_4 N_3^2 \tag{62}$$

$$Nu = \frac{\alpha L}{k} = \frac{1}{|1 - T_A^*|}\left(N_3 T^* - \frac{dT^*}{dy^*}\right) \tag{63}$$

where

$$N_3 = \frac{5\,k_B\,j\,L}{2k\,e}, \qquad N_4 = \frac{4}{25}\frac{e^2k}{k_B^2\,\sigma\,T_c} \tag{64}$$

The boundary conditions for the cathode and anode are:

For the cathode:

$$y^* = 0, \qquad T^* = 1 \tag{65a}$$

For the anode:

$$y^* = 1, \qquad T^* = T_A^* \tag{65b}$$

The solution of Eq. (62) is

$$T^* = (T_A^* - N_3N_4 - 1)\frac{1 - \exp N_3y^*}{1 - \exp N_3} + (1 + N_3N_4y^*) \tag{66}$$

The two relations expressing the Nusselt numbers are:

For the cathode:

$$Nu_c = \frac{N_3}{(1 - T_A^*)}\left(\frac{T_A^* - N_3N_4 - 1}{1 - \exp N_3} + 1 - N_4\right) \tag{67}$$

For the anode:

$$Nu_A = \frac{N_3}{(1 - T_A^*)} \left(\frac{T_A^* - N_3 N_4 - 1}{1 - \exp N_3} \exp N_3 + T_A^* - N_4 \right) \tag{68}$$

For very small currents ($j \to 0$), N_3 becomes zero and Eqs. (65) through (68) reduce to

$$T^* = 1 + y^* (T_A^* - 1), \qquad Nu_c = Nu_A = 1 \tag{69}$$

A parameter that includes the Nusselt number and temperature, $Nu(1 - T_A^*)$, is plotted in Fig. 5 for the cathode and the anode vs T_A^* for different values of N_3 and N_4. Values were determined from Eqs. (67) and (68). Typical numerical values of N_3 and N_4 may be calculated, for example, by considering the distance between the electrodes to be $L = 10^{-2}$ m, the current density to be $j = 5 \times 10^5$ A/m^2, the thermal conductivity of the gas (assuming it is argon) to be $k = 0.5$ J/m-s-°K, with an electrical conductivity $\sigma = 10^4$ A/V-m, and a cathode temperature $T_c = 3000$°K. The values of N_3 and N_4 are then computed to be $N_3 = 2.1$ and $N_4 = 0.36$.

Computation of the temperature profile and Nusselt number was done with the values of N_3 in the range of 0 to 6 and with the values of N_4 in the range of 0.1 to 0.5. In Fig. 5, two values of N_3 were chosen to be 0.4 and 2.0 and two values of N_4 to be 0.1 and 0.5. For a given T_A^*, the parameter $Nu(1 - T_A^*)$ is a function of (N_3/N_4) for the cathode and a function of $(N_3 \times N_4)$ for the anode. In a given channel of width L and cathode temperature T_c, an increase in N_3 at constant N_4 may be accomplished by an increase in the current density, whereas comparisons over a range of N_4 with constant N_3 would normally reflect a comparison of different gases.

The larger values of $Nu(1 - T_A^*)$ for the anode than for the cathode (see Fig. 5) result from changes in temperature distributions across the channel. The analysis indicates that the relative value of anode-to-cathode temperature $T_A^* = T_A/T_c$ is very important. In actual practice, the temperature of the anode is generally much lower than that of the cathode because the anode is cooled and thermionic emission is allowed to occur at the cathode; therefore, $T_A^* < 1$. In arc-plasma devices, a reasonable value of T_A^* is 0.2. Actually, consideration of sheath and surface effects (caused, for example, by the cathode and anode fall regions, as well as the emission work on the surface, or work function) will result in a much higher heat flux for the anode and much lower

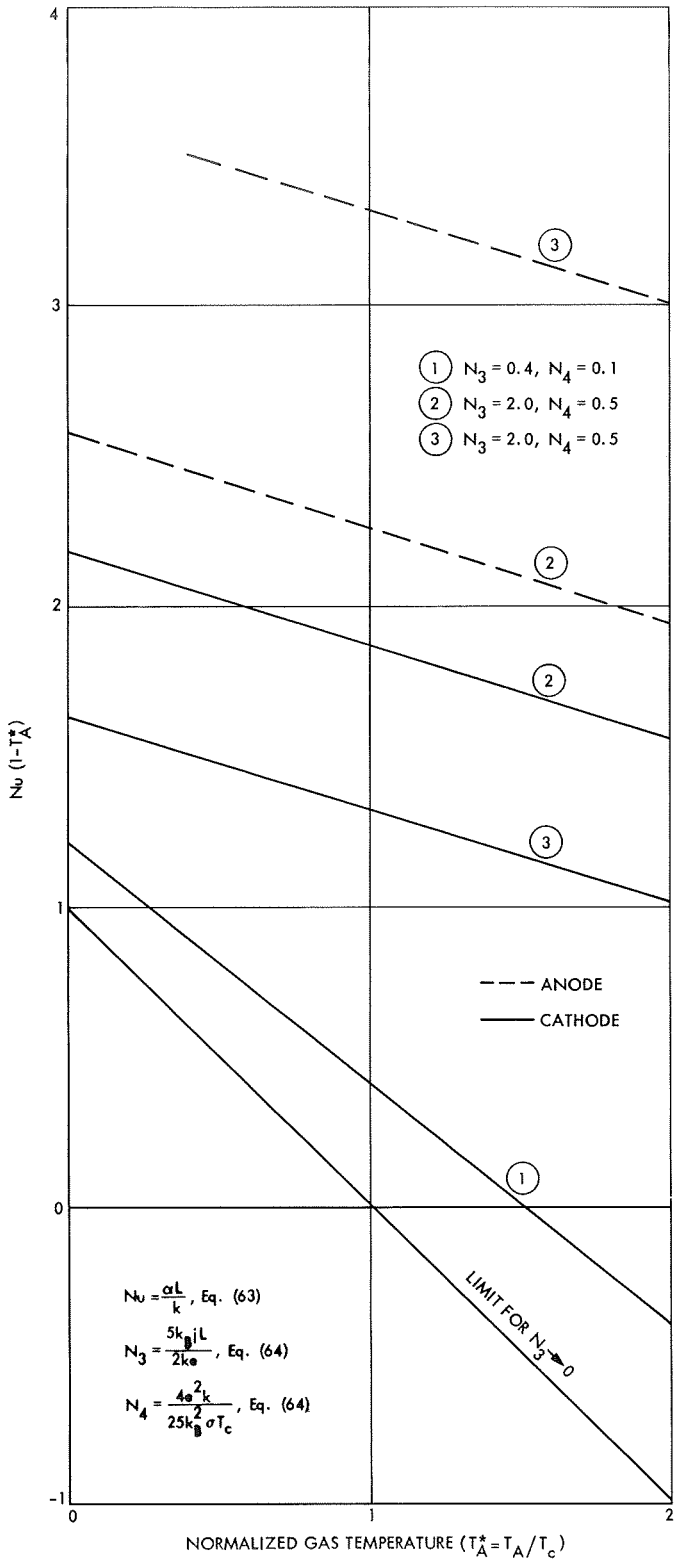

Fig. 5. $Nu\,(1 - T_A^*)$ vs T_A^* for $N_3 = 0$, 0.4, and 2.0 and $N_4 = 0.1$ and 0.5

values at the cathode than those computed from Eqs. (61) and (63) and the Nusselt relations given by Eqs. (67) and (68). A method that takes the surface and sheath effects into consideration is described in Section III.

For equal temperatures of the cathode and the anode ($T_A^* = 1$), the Nusselt number approaches infinity and $Nu(1 - T_A^*)$ can be computed from Eqs. (67) and (68). However, it is not possible to compute the heat flux from the Nusselt number for $T_A^* = 1$; therefore, for this case, the heat flux must be computed directly from the wall temperature and the temperature gradient at the wall, using Eq. (61).

The effect of T_A^* on the temperature distributions across the channel, computed from Eq. (66), is shown in Fig. 6 for typical values of N_3 and N_4 (namely, $N_3 = 4$ and $N_4 = 0.3$). However, when $N_3 = 0$, the temperature distribution is independent of N_4, which is shown by Eq. (66). For experimental purposes, it is important that $T_A^* < 1$, not only to enable thermionic emission at the cathode, but also to make it easier to measure the change in temperature distribution caused by a change in the current flow, as the influence of the current is greater under these conditions. For the limiting case of $N_3 = 0$, that is, the current density $j = 0$, the temperature distribution across the channel for all values of N_4 is linear, as shown by Eq. (69); the heat transfer reduces to pure conduction so that $Nu_c = Nu_A = 1$.

For a typical value of $T_A^* = 0.2$, the temperature distribution across the channel is shown in Figs. 7 and 8 for different values of N_3 and N_4. It may be observed more clearly in Fig. 8 that, when the anode temperature is lower than that of the cathode, a reversal in the sign of the temperature gradient can occur at the cathode ($y^* = 0$). For example, when $N_3 = 2.0$ and $N_4 = 0.5$, the gas temperature in the vicinity of the cathode is raised sufficiently by joule heating for the temperature gradient to be positive; hence, heat transfer by convection occurs from the gas to the cathode. However, when N_4 is reduced to 0.1, the gas temperature is lower than that of the cathode surface, and heat is transferred by convection from the cathode to the gas. It should be recalled that such a comparison of different values of N_4 at a constant value of N_3 infers a comparison of different gases because N_4 is related to gas properties and is independent of the current density. For a typical gas with given N_4 (e.g., $N_4 = 0.3$), a similar reversal of temperature gradient at the cathode is observed when the current density is raised sufficiently to bring N_3 from 0 to 4.

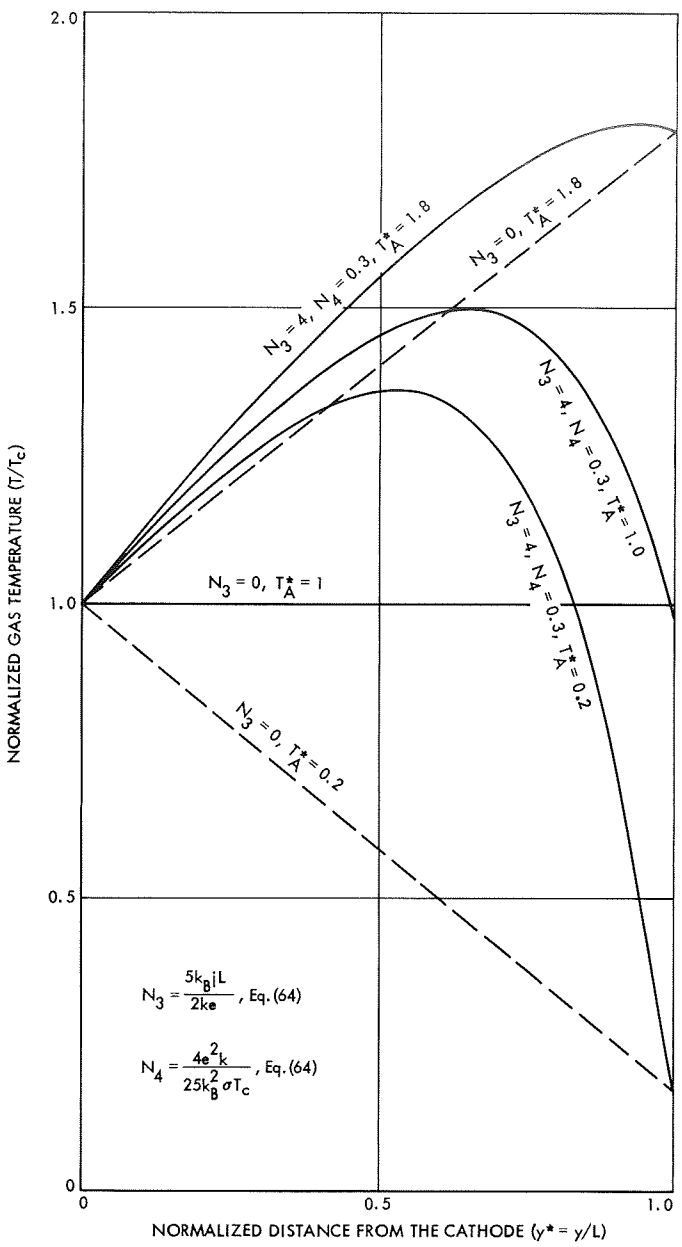

Fig. 6. Effect of relative anode temperature T_A^* on the temperature distribution across the channel

VI. Summary and Conclusions

This report presents a comparatively general analysis of heat transfer for a two-temperature gaseous plasma in the presence of electromagnetic fields. A singly ionized, quasineutral plasma is assumed in which the properties are variable and the flow is laminar. The total velocity of the electrons is considered to be the sum of the mass averaged directed velocity of the gas mixture plus an ambipolar-diffusion velocity resulting from the concentration gradient of the electrons plus a field velocity of

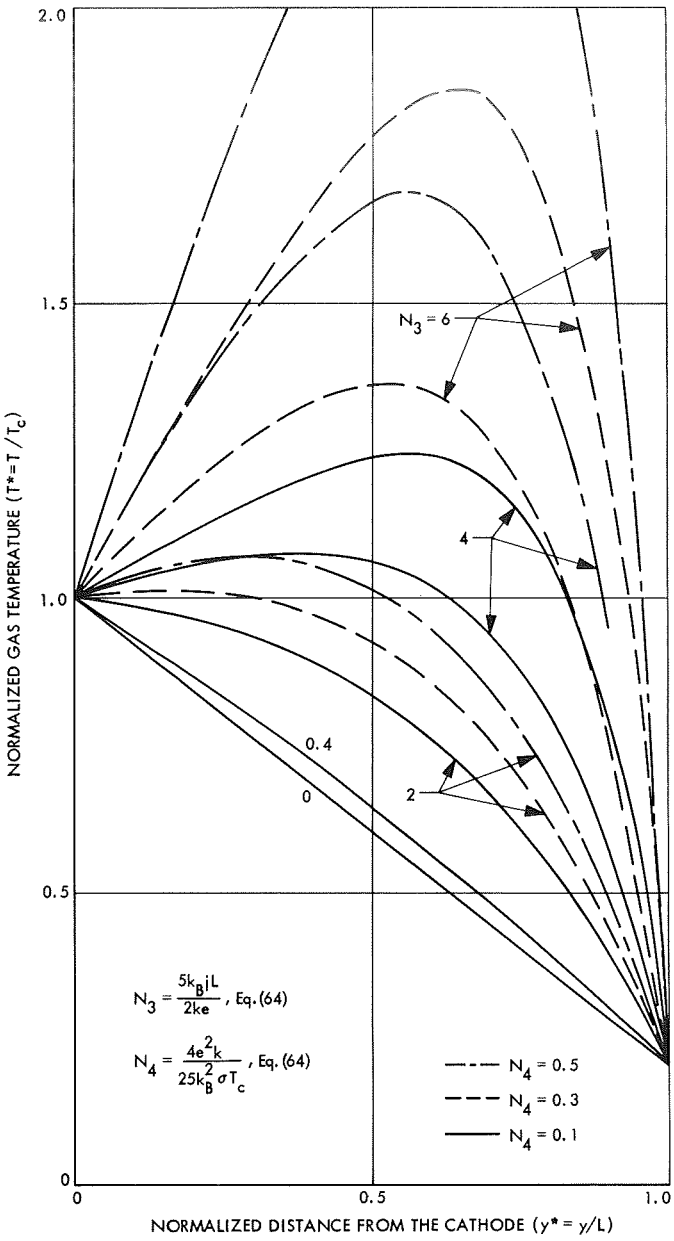

Fig. 7. Temperature distribution across the channel for $T_A^* = 0.2$

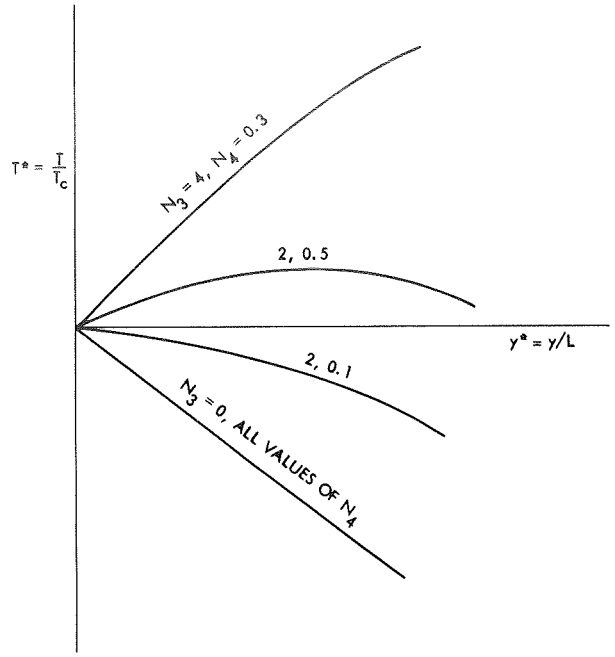

Fig. 8. Temperature distribution in the vicinity of the cathode for $T_A^* = 0.2$

the electrons in an electromagnetic field. The field velocity for ions is assumed to be negligible.

It has been shown that the Nusselt number depends upon six different dimensionless parameters (Eq. 57) compared to two parameters for a nonionized, low-temperature gas flow without applied electromagnetic fields. The total heat flux to the wall consists of the convective heat flux (which can be computed from Nusselt's relations) plus additional terms representing energy loss or gain at the sheath edge near the surface.

A sheath analysis has been presented for a species in an accelerating field, in a decelerating field, emitted from the wall, and recombining at the wall. Expressions for the energy loss or gain terms are then obtained for special cases of a cathode, an anode, and some other surfaces. The total heat flux for the anode has been found to be the same as that derived semiempirically by Eckert and Pfender (see Ref. 18).

A simple heat-transfer model consisting of flow between parallel flat plates was then considered to show the importance of different nondimensional parameters (Eq. 64) on convective heat flux. The current was assumed to be uniformly distributed and the thermophysical properties were assumed to be constant. The temperatures of each of the species were taken to be equal. The distribution of the gas temperature between electrodes was found to be dependent upon a dimensionless variable N_3, which is proportional to the current, and on another dimensionless variable N_4, which is inversely proportional to the cathode temperature and directly proportional to the ratio of thermal-to-electrical conductivity.

The ratio of the anode-to-cathode surface temperatures was also found to be important. For a typical value of the ratio of these temperatures ($T_A^* = 0.2$), it has been shown that a reversal in the sign of the convective heat transfer can occur at the cathode by independently adjusting the value of N_4, as well as by independently adjusting the value of N_3. In a physical sense, the reversal in the convective heat flux to and from the cathode is brought about by a change in the joule heating that influences the temperature gradient at the surface. Changes in N_4 to accomplish this reflect comparisons of different gases because the thermophysical properties are involved, whereas changes in N_3 reflect adjustments in current density for a given gas.

Nomenclature

$\mathbf{B}$	magnetic induction, V/s-m^2
D	diffusion coefficient, m^2/s
D_{amb}	ambipolar diffusion coefficient, m^2/s
E	internal energy, J/kg
E^o	total energy = $E + V^2/2$, J/kg
$\mathbf{E}'_f$	externally applied electric field, V/m
e	elementary charge = 1.602×10^{-19} A-s
$\mathbf{F}$	volume force, N/m^3
g_j	species mass-density ratio = ρ_j/ρ
$\mathbf{H}$	magnetic field, A/m
h	enthalpy, J/kg
I_i	ionization potential, eV
I_{mi}	ionization potential per unit mass ion, J/kg$_i$
i	degree of ionization
$\mathbf{j}$	current density, A/m^2 (electron current density that is considered to be positive)
k	thermal conductivity coefficient, J/m-°K-s
k_B	Boltzmann constant = 1.38×10^{-23} J/°K
L	a characteristic length
M	mass of particle, kg
m	mol mass, kg/kmol
m_R	mass rate of production, kg/m^3-s
N	dimensionless number (Eqs. 58 and 64)
n	number density, m^{-3}
$\dot{\mathbf{n}}$	flux of particles, m^{-2}s^{-1}
Nu	Nusselt number
Pr	Prandtl number
p	pressure, bar
Q_{jc}	energy transferred to jth species by molecular encounter, J/m^3-s
Q_{jf}	field energy, J/m^3-s
$Q_{j,chem}$	chemical energy carried away by jth species, J/m^3-s
$\mathbf{q}$	heat flux, J/m^2-s
$\mathbf{q}_b$	convective heat flux at b, J/m^2-s
$\mathbf{q}_R$	radiative heat flux, J/m^2-s
R	reaction rate, m^{-3}s^{-1}
R^*	universal gas constant = 8314 J/kmol-°K
Re	Reynolds number
Sc	Schmidt number = $\rho D/\eta$
T	temperature, °K
u	a characteristic velocity, m/s
$\mathbf{V}$	fluid velocity, m/s
$\mathbf{V}'_{dj}$	diffusive velocity of jth species, m/s
$\mathbf{V}'_{fj}$	electromagnetic field velocity of jth species, m/s
$\mathbf{V}_j$	velocity of jth species, m/s
$\mathbf{V}'_j$	relative velocity of jth species, m/s
x_j	mol-fraction of jth species = n_j/n
x,y	coordinate directions, m
Z	partition function
α	convective heat-transfer coefficient, J/m^2-s-°K
Γ	collision frequency, m^{-3}s^{-1}
Γ'	collision frequency of one molecule, s^{-1}
δ	Kronek's delta (Eq. 15)

Nomenclature (contd)

ϵ_R	radiative energy, J/m³-s
η	dynamic viscosity, kg-m/s
θ	temperature ratio $= T_e/T_h$
λ	mean free path, m
λ_D	Debye shielding distance, m
μ	mobility coefficient, m²/V-s
ρ	density, kg/m³
ρ_{el}	charge density, A-s/m³
σ	electrical conductivity, A-V/m
τ	stress tensor
ϕ	dissipation function (Eq. 25)
ϕ_w	work function of surface material, V
φ_A	anode falls, V
φ_w	potential drop in sheath
∇	vector operator

Subscripts and superscripts

A	anode
a	atoms
b	condition at one mean free path from body surface
c	cathode
e	electrons
f	in the presence of a field
h	heavy particles
i	ions
j	any species
r,s	coordinate directions
s	sheath edge condition
w	wall condition
$*$	dimensionless quantities

References

1. Gruszczynski, J. S., and Warren, W. R., "Experimental Heat Transfer Studies of Hyper Velocity Flight in Planetary Atmospheres," *AIAA J.*, Vol. 2, p. 1542, 1964.
2. Rose, P. H., and Stankevics, J. O., "Stagnation Point Heat Transfer Measurements in Partially Ionized Air," *AIAA J.*, Vol. 1, p. 2752, 1963.
3. Park, C., "Heat Transfer from Non-equilibrium Ionized Argon Gas," *AIAA J.*, Vol. 2, p. 169, 1964.
4. Okumo, A. F., and Park, C., *Convective Stagnation Point Heat Transfer in Partially Equilibrium Flow of Highly Ionized Nitrogen*, NASA-TM-X-61187. National Aeronautics and Space Administration, Washington, 1968.
5. Bade, W. L., "Stagnation Point Heat Transfer in a High Temperature Inert Gas," *Phys. Fluids*, Vol. 5, pp. 150–154, Feb. 1962.
6. Back, L. H., *Effects of Surface Cooling and Heating on Structure of Low-Speed, Laminar Boundary-Layer Gas Flows With Constant Free-Stream Velocity*, Technical Report 32-1301. Jet Propulsion Laboratory, Pasadena, Calif., Aug. 1968.

References (contd)

7. Back, L. H., *Laminar Boundary-Layer Heat Transfer from a Partially-Ionized Monatomic Gas by the Similarity Approach,* Technical Report 32-867. Jet Propulsion Laboratory, Pasadena, Calif., Dec. 15, 1965.

8. Mirels, H., and Welsh, W. E., Jr., "Stagnation Point Boundary Layer with Large Wall to Free Stream Enthalpy Ratio," *AIAA J.*, Vol. 6, No. 6, pp. 1105–1110, June 1968.

9. Mirels, H., "Subsonic Flow of Hot Gas Through a Highly Cooled Channel," *AIAA J.*, Vol. 6, No. 8, pp. 1585–1587, Aug. 1968.

10. Bose, T. K., "Der Waermeuebergang von Argon- und Stickstoff-plasma an eine kalte Wand, Diss.," *Tech. Univ.*, Stuttgart, West Germany, 1965. Also in *Proceedings of the Energy Conversion, Electric Propulsion and Plasma Flows Conference,* DLR-67-17. Stuttgart, Oct. 1967.

11. Penski, K., "Zustands- und Transportgroessen von Argon Plasma," *Chem. Ing. Tech.*, Vol. 34, pp. 84–86, 1962.

12. Uhlenbusch, J., "Berechnung der Materialfunctionen eines Stickstoff und Argon Plasmas aus gemessenen Bogendaten," *Z. Phys.*, Vol. 179, p. 347, 1964.

13. Bosnjakovic, F., unpublished data, Institut fuer Thrmodynamik, Technical University, Stuttgart, Germany.

14. Kerrebrock, J. L., "Conduction in Gases with Elevated Electron Temperature," in *Engineering Aspects of Magnetohydrodynamics,* pp. 327–346, Columbia University Press, New York, 1962.

15. Monti, R. and Napolitano, L. G., "Generalized Saha Equation for Non-equilibrium Two Temperature Plasmas," in *Proceedings of the Fifteenth International Astronomical Congress,* 1964.

16. Veis S., "The Saha Equation and Lowering of the Ionization Energy for a Two-Temperature Plasma," in *Proceedings of the Fourth Czechoslovakian Conference on Electronics and Vacuum Physics,* Oct. 12–17, 1968.

17. Kerrebrock, J. L., "Electrode Boundary Layers in D.C. Plasma Accelerators," *J. Aerosp. Sci.*, pp. 631–643, Aug. 1961.

18. Eckert, E. R. G., and Pfender, E., "Advances in Plasma Heat Transfer," in *Advances in Heat Transfer: Volume 4,* pp. 229–316. Academic Press, New York, 1968.

19. Shih, K. T., et al., "Experimental Studies of the Electrode Heat Tranfer in an MPD Arc Configuration," Paper 67-673, presented at the AIAA Conference on Electric Propulsion and Plasma Dynamics, Colorado Springs, Colo., Sept. 11–13, 1967.

20. Shih, K. T., et al., "Experimental Anode Heat Transfer Studies in a Coaxial Arc Configuration," *AIAA J.*, Vol. 6, No. 8, pp. 1482–1487, Aug. 1968.

21. Sherman, A., and Reshotko, E., "The Nonequilibrium Boundary Layer Along a Channel Wall," Paper 68-134, presented at the AIAA Sixth Aerospace Sciences Meeting, New York, 1968.

References (contd)

22. Weizel, W., and Rompe, R., *Theorie Elektrischer Lichtbögen und Funken,* Leipzig, 1949.

23. Sutton, G. W., and Sherman, A., *Engineering Magnetohydrodynamics,* McGraw-Hill Book Co., Inc., New York, 1965.

24. Bose, T. K., *Experimental and Theoretical Studies on Electrostatic Probes,* HTL-TR-83. Heat Transfer Laboratory, University of Minnesota, Minneapolis, Minn., May 1968.

25. Fay, J. A., "Hypersonic Heat in Air Boundary Layer," in *High Temperature Aspects of Hypersonic Flow,* pp. 583–605. Edited by W. C. Nelson. The Macmillan Company, New York, 1964.

26. Jukes, J., *Heat Transfer from Highly Ionized Argon Produced by Shock Waves,* masters thesis, Cornell University, Ithaca, N.Y., June 1956.

27. Cobine, J. D., *Gaseous Conductors,* Dover Publications, Inc., New York, 1958.

28. Cheng, F. F., *Electric Probes in Plasma Diagnostic Techniques.* Edited by R. H. Huddlestone and S. L. Leonard. Academic Press, New York, 1965.

NASA — JPL — Coml., L.A., Calif.